

Electrochemical Reduction of Carbon Dioxide III. The Role of Oxide Layer Thickness on the Performance of Sn Electrode in a Full Electrochemical Cell

Jingjie Wu, Frank G. Risalvato, Shuguo Ma and Xiao-Dong Zhou

Department of Chemical Engineering, University of South Carolina, Columbia,
South Carolina 29208, USA

Supporting Information

Index	Page
Experimental	S2-S5
Figure S1. XPS of native and annealed Sn nanoparticles.	S6
Figure S2. Auger spectra of etched Sn GDE, native and annealed Sn particles.	S7
Figure S3. Linear scan voltammetry of Sn GDE annealed at 180 °C for 24 h before and after pre-electrolysis.	S8
Figure S4. XRD pattern of commercial SnO and SnO ₂ powders.	S9
Figure S5. XPS of commercial SnO and SnO ₂ powders.	S10
Figure S6. Cyclic voltammetry of SnO ₂ GDE before and after pre-electrolysis at -2 V for 30 min.	S10
Figure S7. Electrochemical activity of commercial SnO and SnO ₂ GDE with pre-electrolysis for CO ₂ reduction at -1.2 V.	S11
Figure S8. Performance of SnO ₂ GDE without pre-electrolysis for CO ₂ reduction at -1.2 V.	S11
Figure S9. XPS characterization and electrochemical activity of etched as-received Sn GDE.	S12

Experimental

Materials. KHCO₃ (99.7%), HCl (37% in water), Nafion perfluorinated resin solution (5 wt.%) and isopropanol (99.5%) were purchased from Sigma-Aldrich; hydrogen (99.999%), argon (99.999%), helium (99.999%), and carbon dioxide (99.999%) were purchased from Airgas; Nafion® 212 membrane was purchased from Dupont; Pt/C (60%) was obtained from Johnson Matthey; Sn nanoparticles (ASP 100 nm) were purchased from Alfa Aesar; the graphite gas diffusion layer (GDL 10 BC) was ordered from SGL group. All chemicals were used without further purification. Electrolyte solutions were prepared with DI water (Siemens, Labstar).

Annealing procedure. 0.2 g of Sn nanoparticles was placed in a muffle or tube furnace (Thermo Scientific) under an air atmosphere at the specified temperature (100~180 °C) and time period (6~24 h). Sn nanoparticles were then allowed to cool slowly to room temperature over several hours.

Electrode preparation. The Sn gas diffusion electrodes (Sn GDEs) were prepared from the native and annealed Sn nanoparticles. In short, a suspension of Sn nanoparticles and Nafion perfluorinated resin solution along with a 50/50 mixture of water and isopropanol were formed by ultrasonication for at least 30 min before being sprayed onto GDLs to form GDEs with a Sn loading of ~2 mg cm⁻². The Sn GDEs were then heat-treated at 130 °C for 30 min in the vacuum oven and allowed to cool slowly back to room temperature before testing. The anode, Pt GDE, with a Pt loading of 0.3 mg cm⁻² was made as the similar procedure as Sn GDE. The Pt GDE was hot-pressed at 130 °C and 50 PSI for 5 min with a Nafion® 212 membrane.

Etching Procedure. GDEs were etched by cathodizing in 1:5 HCl : H₂O solution at -3.0 V for 5 min as described.

Full electrochemical cell testing. The electrochemical test was carried out in a custom-designed full electrochemical cell with a circulating aqueous electrolyte buffer layer. The cell consists of an anode electrode (Pt GDE), an ion conducting membrane (Nafion® 212), an aqueous electrolyte buffer layer, and a cathode electrode (Sn GDE). The Nafion® 212 membrane separates the anode electrode of Pt GDE from the electrolyte. The cell ran at T=298.15K and P⁰=1.013 bar. An electrolyte of 0.1 M KHCO₃ was pumped through the buffer layer at a rate of 7 mL/min. The anode side of the full electrochemical cell was supplied with H₂ at a rate of 150 ml min⁻¹. The cathode side of the full electrochemical cell was supplied with CO₂ at a rate of 45 ml min⁻¹. The electrolysis was conducted under a constant cell potential of -1.2 V for 2 hours by employing a potentiostat/galvanostat (Solartron 1470E) after first reducing each Sn GDE under Ar for 30 minutes at -2.0 V. Tests were also conducted at constant potentials for 30 minutes to analyze the GDEs selectivity towards the formation of CO and HCOO⁻ over the potential range from -0.8 V to -2.0 V. In order to verify the removal of SnO_x after pre-electrolysis, linear scan voltammetry or cyclic voltammetry was conducted from 0 V to -2.0 V at 50 mV s⁻¹ with Ar supplying to the cathode. The individual electrode potential during potentiostatic electrolysis was measured by using a Ag/AgCl reference electrode which was placed in the middle of the buffer layer. In order to correct internal resistance (IR) drop, the ohmic resistance between the cathode and reference electrode was measured by using electrochemical impedance spectroscopy at open circuit voltage, with an amplitude of 5 mV and frequency range from 100 kHz to 0.1 Hz.

Product measurement and quantification. Liquid products were quantified using 1D ¹H nuclear magnetic resonance (NMR) spectroscopy. The NMR data was acquired using a Varian Mercury/VX 400 MHz spectrometer using the WET solvent suppression pulse sequence. Standard curves were made using purchased formic acid over the concentration range of interest,

with the internal standards sodium 3-(trimethylsilyl) propionate 2, 2, 3, 3-d (4) (TSP), in 0.1 M KHCO₃. NMR parameters used were identical between collected spectra to make standard curves and in the subsequent quantification of products in the electrolyte. The spectra were measured at room temperature with an acquisition time of 2.18 s, a relaxation delay of 20 s, and 32 free induction decay averages. A 6 mM concentration of internal standard TSP solution was prepared in D₂O. NMR samples were prepared by withdrawing 500 µL of product solution from the electrolysis cell and depositing it into an NMR tube followed by adding 100 µL of TSP internal standard solution. The ratio of the area of the formate peak to the area of the TSP peak was compared to standard curves to quantify the concentrations of the reaction products. The coulombs needed to produce that concentration of formate was calculated and divided by the total coulombs passed during the chronoamperometry to determine the Faradaic efficiency of formate.

Gas products were quantified by using gas chromatography (GC). The reactant CO₂ and product gases from the outlet of the cathodic compartment were vented directly into the gas-sampling loop of the GC (Inficon Micro 3000 GC). A GC run was initiated every 10 minutes. The GC had two channels, one equipped with a packed 10 m MolSieve 5A column and the other with a packed 8 m Plot Q column. Each channel was connected with a thermal conductivity detector (TCD). Helium (Airgas, 99.999%) was used as the carrier gas to quantify CO concentration while argon (Airgas, 99.999%) was used to quantify hydrogen concentration. A standard gas mixture consisting of 1000 ppm CO and 1000 ppm H₂ in CO₂ was employed to calibrate the GC to get the gas peak area conversion factor. The moles of CO that produced in the course of electrolysis reaction were calculated from the GC peak area as follows:

$$n_{CO} = \frac{\text{peak area ratio}}{\alpha} \times \text{flow rate} \times \text{electrolysis time} \times \frac{P^0}{RT}$$

where α is a conversion factor based on calibration of the GC with a standard sample, $p^0 = 1.013$ bar, $T = 273$ K, and R universal gas constant. Flow rate of CO_2 was corrected to standard temperature and pressure.

Physical characterization. High-resolution transmission electron microscopy (HRTEM) images were acquired with a JEM-2100F TEM with a field-emission gun. Powder X-ray diffraction (XRD) patterns were collected by a Rigaku/Miniflex diffractometer with Cu K radiation detector. X-ray photoelectron spectra (XPS) were obtained with a PHI Versa Probe II Scanning XPS Microprobe. The oxide layer thickness can be calculated using the calculations of the type developed by Strohmeier and Carlson defined as follows:

$$d = \lambda_{\text{ox}} \sin \theta \ln \left(\frac{N_m \lambda_m I_{\text{ox}}}{N_{\text{ox}} \lambda_{\text{ox}} I_m} + 1 \right)$$

where θ is the photoelectron take-off angle (90°), λ_{ox} and λ_m are the inelastic mean free path (IMFP) of the oxide and metal, I_{ox} and I_m are the area percentages of the oxide and metal peaks from the high-resolution spectrum, and N_m and N_{ox} are the volume densities of the metal atoms in the metal and oxide, respectively. The IMFP can be acquired from NIST Electron Inelastic-Mean-Free-Path Database.

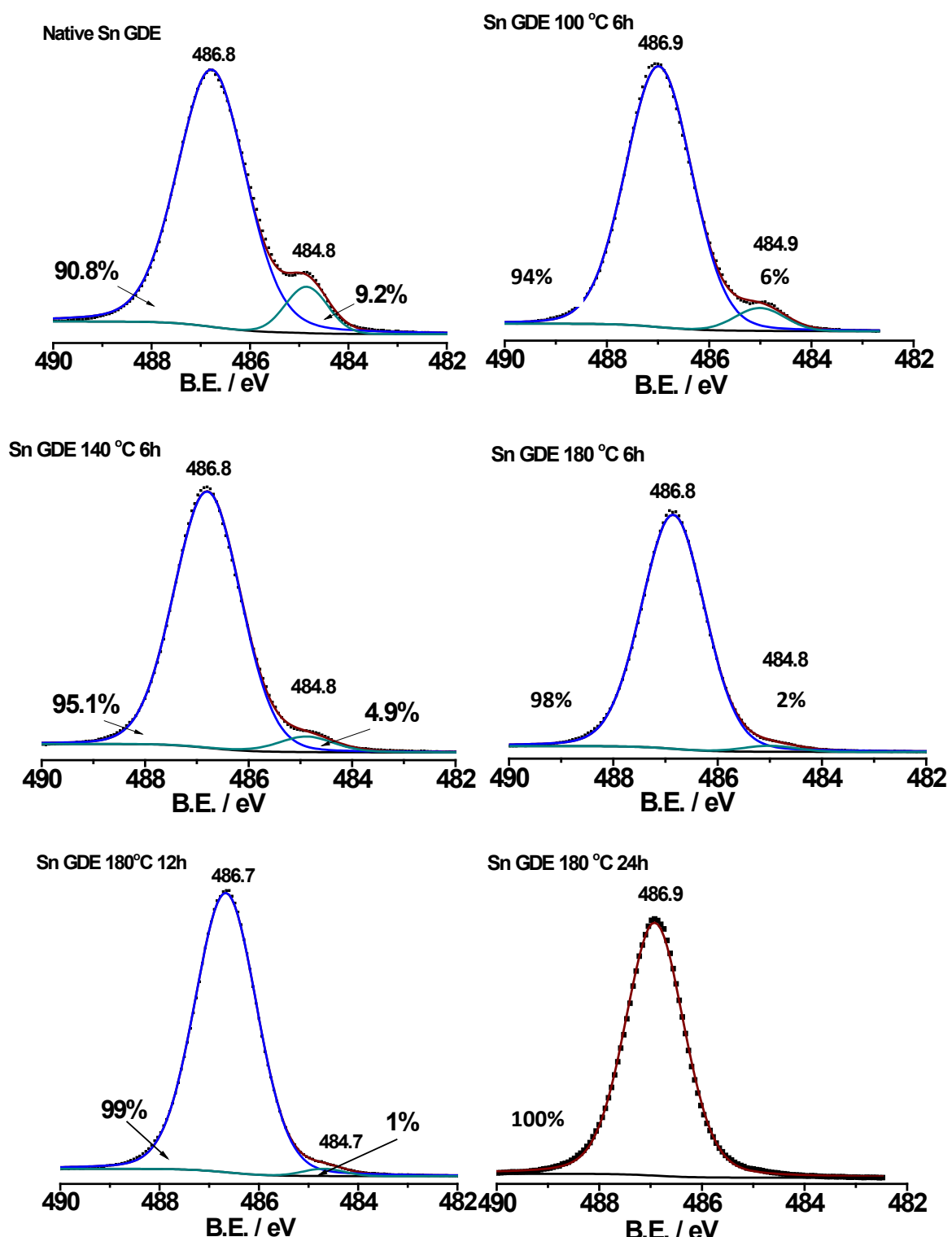


Figure S1. XPS of native and annealed Sn nanoparticles.

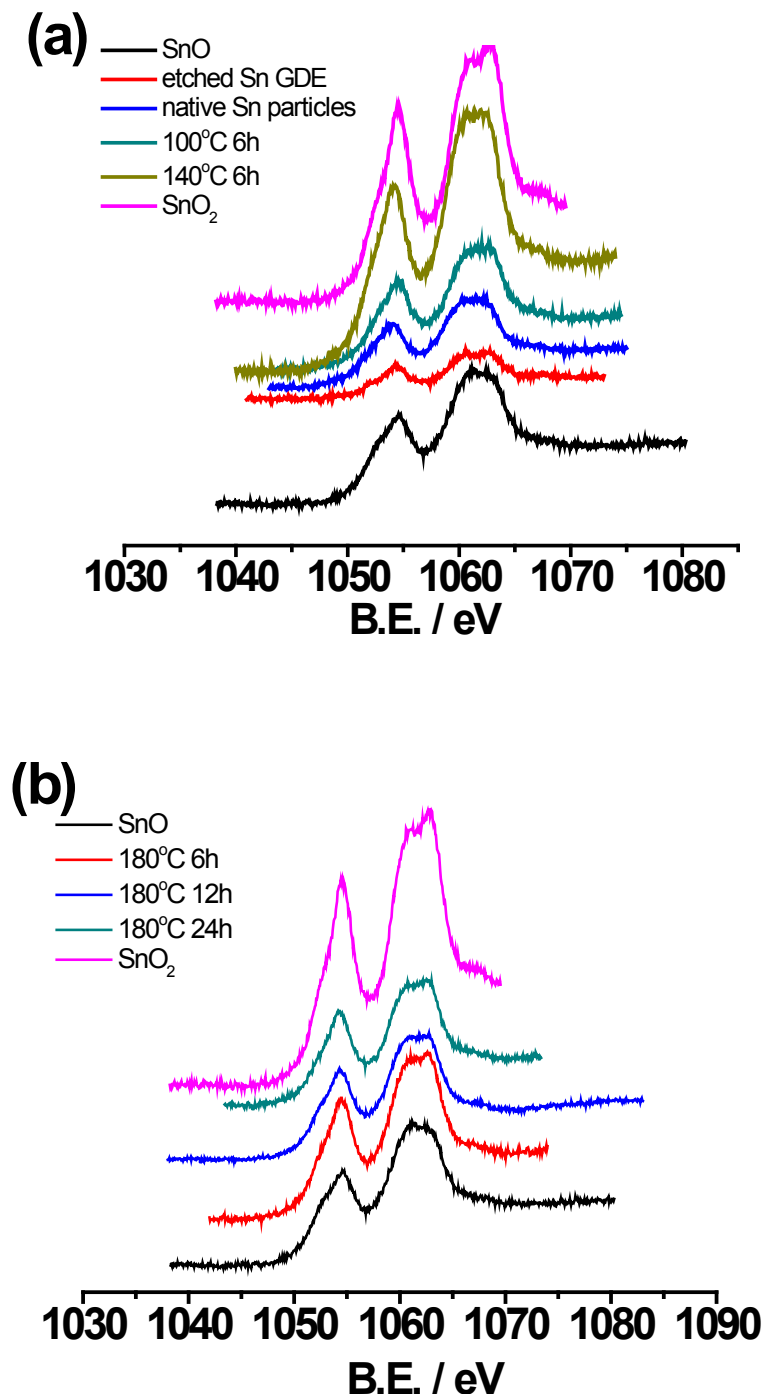


Figure S2. Auger spectra of etched Sn GDE, and native and annealed Sn particles together with commercial SnO and SnO₂ particles.

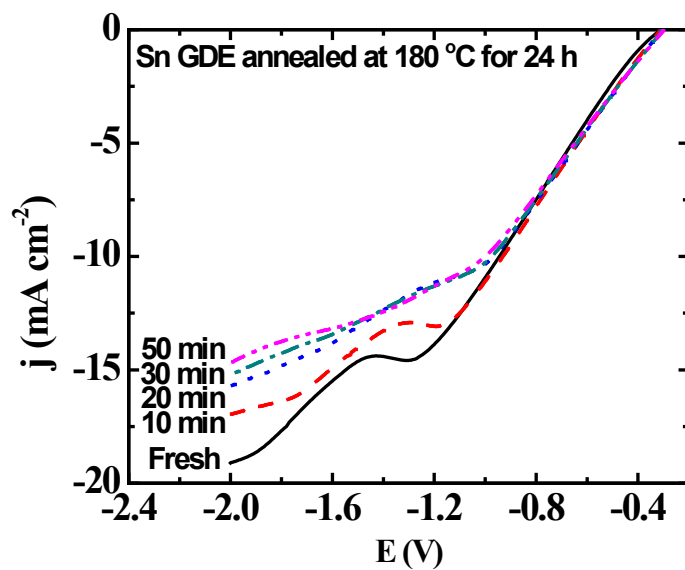


Figure S3. Linear scan voltammetry of Sn GDE annealed at 180 °C for 24 h before and after pre-electrolysis for a variety of duration. The SnO_x scale was removed after pre-electrolysis for 20 min at -2 V under Ar.

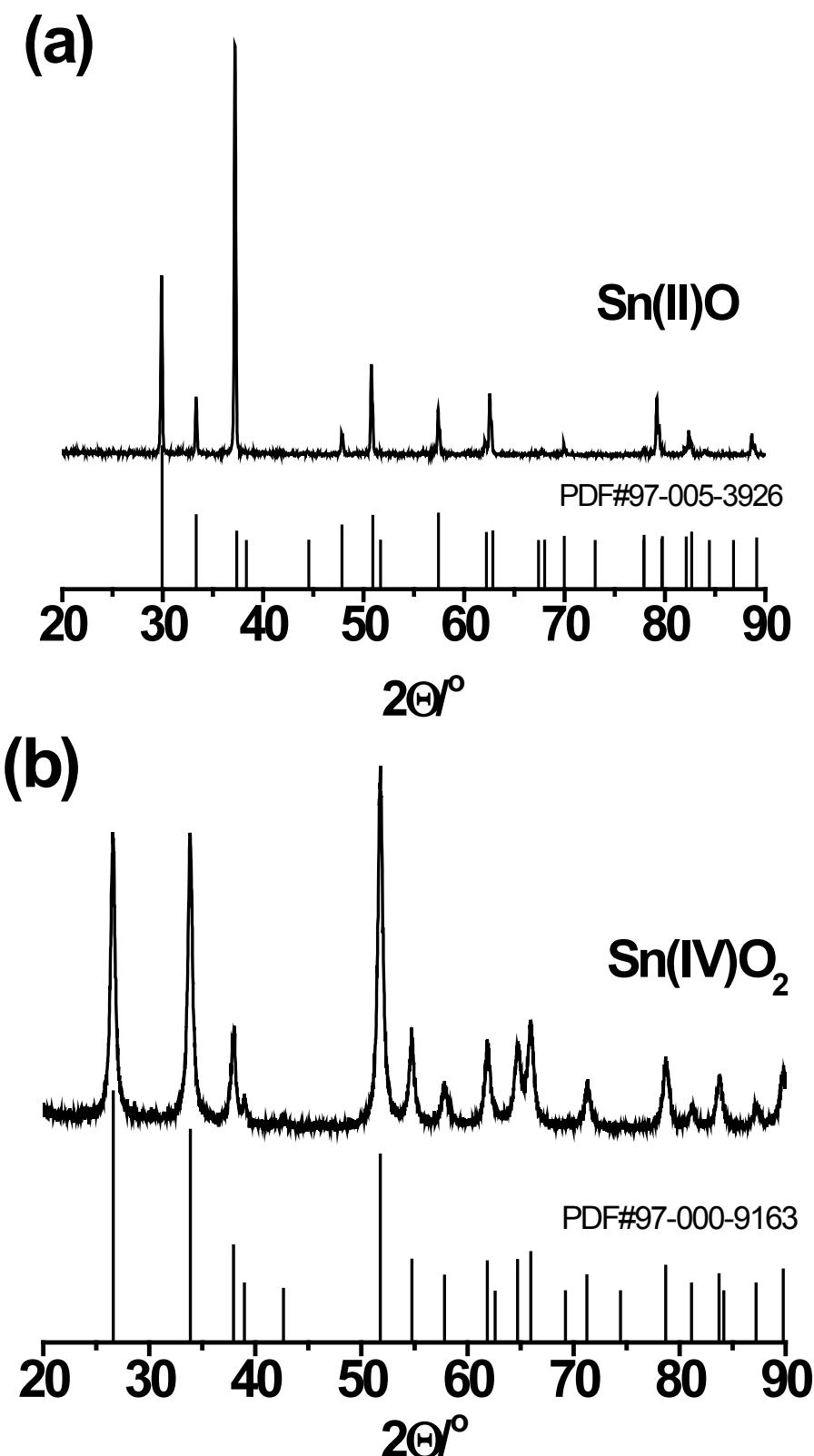


Figure S4. XRD pattern of commercial (a) Sn(II)O and (b) Sn(IV)O₂ powders.

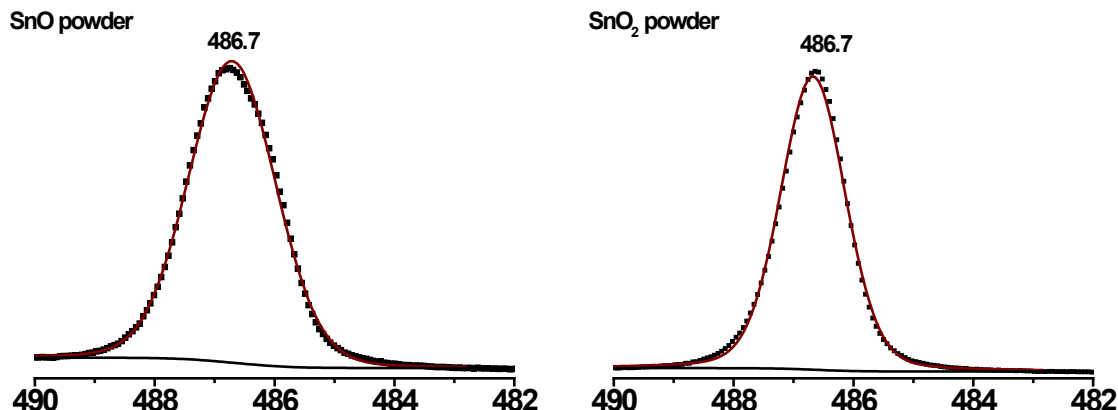


Figure S5. XPS of commercial (a) Sn(II)O and (b) Sn(IV)O₂ powders.

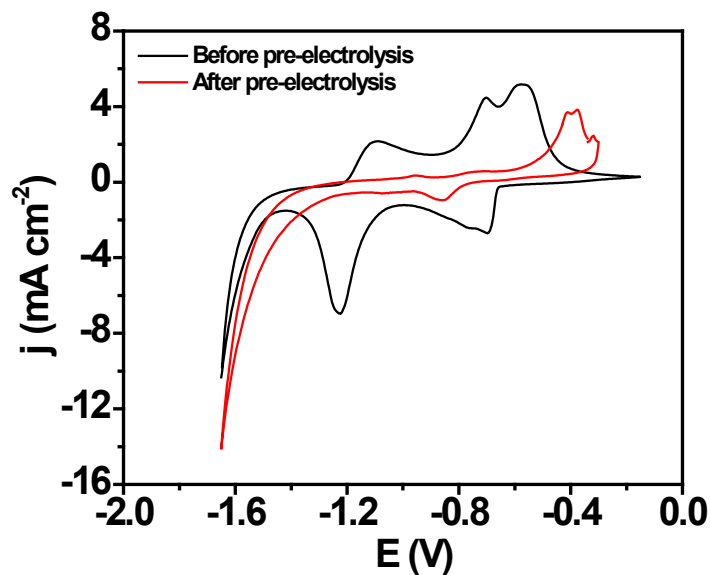


Figure S6. Cyclic voltammetry of SnO₂ GDE before and after pre-electrolysis at -2 V for 30 min. Scan rate is 50 mV s⁻¹.

Tin is a poor metal with a higher electronegativity than most transition metals. At room temperature, tin possesses a native oxide layer, which prevents further oxidation. Cyclic voltammetry measurements showed that this oxide layer was removed at -2.0 V for 30 minutes before we carried out the reduction reaction (See Figure S6). Cyclic voltammetry measurements showed that the oxide was reduced after being kept at -2.0 V for 30 minutes before we carried out the CO₂ reduction reaction.

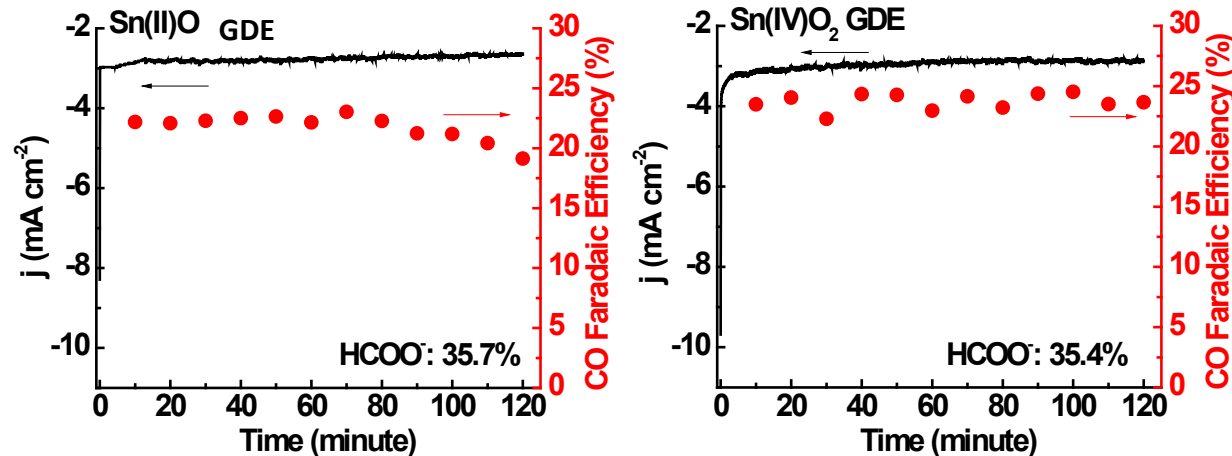


Figure S7. Electrochemical activity of commercial SnO (left) and SnO_2 (right) GDE for CO_2 reduction at -1.2 V. Before initiating CO_2 reduction, both electrodes were reduced at -2 V for 30 min with Ar supplied to the cathode.

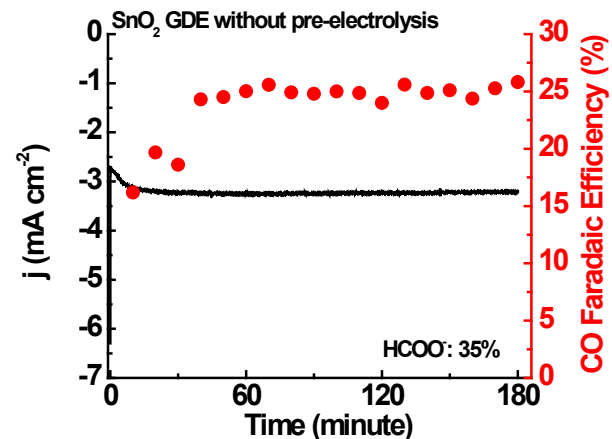


Figure S8. Performance of SnO_2 GDE without pre-electrolysis for CO_2 reduction at -1.2 V.

If Sn-based GDE was used without pre-electrolysis, the reduction reactions of tin oxide to Sn and CO_2 to CO and formate occurred simultaneously. The Faradaic efficiency towards the formation of formate was about 35% at the end of electrolysis and the Faradaic efficiency of CO increased in the first hour operation and then reached to $\sim 25\%$. The Faradaic efficiencies are similar to those of SnO_2 GDE with pre-electrolysis. Hence, the contribution of the SnO_x towards improvement of the activity of Sn particles is negligible.

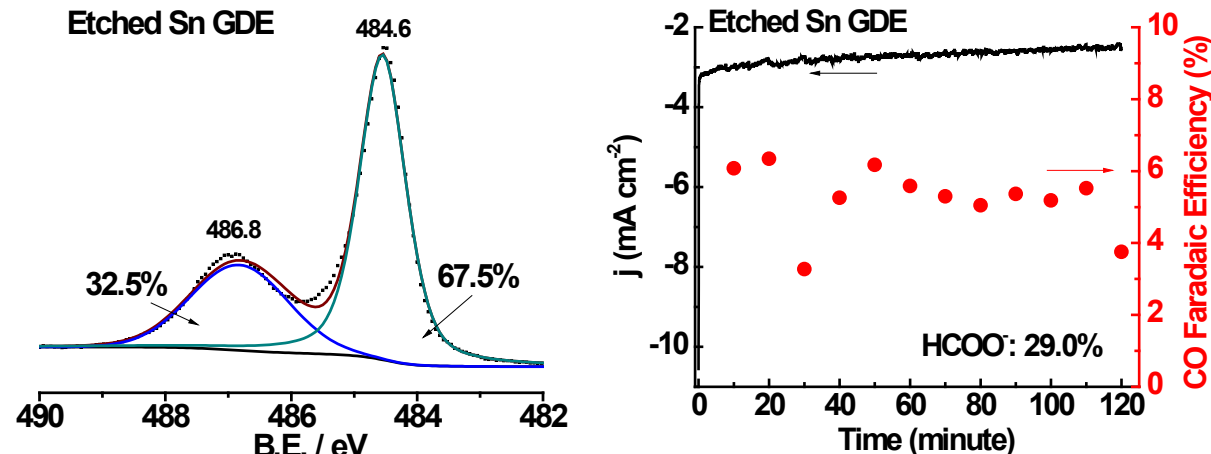


Figure S9. XPS (left) and electrochemical activity for CO_2 reduction catalysis at -1.2 V (right) of etched as-received Sn GDE.

After etching, the XPS shows the atomic ratio of $\text{SnO}_x : \text{Sn}^0$ was reduced to 33 : 67 which corresponds to a 2.0 nm SnO_x layer. The etched Sn GDE exhibited much lower FE for CO ($\sim 5.6\%$) and HCOO^- (29%) under the same electrolysis condition, while no significant difference in the current density. The similar phenomenon of reduced activity towards CO and HCOO^- was also observed in etched Sn foil electrodes. The decline of activity towards CO_2 reduction may result from the increasing of low-coordination number Sn sites present on freshly nucleated Sn clusters following etching, which enhanced H_2 evolution.